



Cite this: DOI: 10.1039/c7cc09809j

Received 4th January 2018,  
Accepted 19th March 2018

DOI: 10.1039/c7cc09809j

rsc.li/chemcomm

## Multicolor GLUT5-permeable fluorescent probes for fructose transport analysis†

 V. V. Begoyan,<sup>a</sup> Ł. J. Weseliński,<sup>a</sup> S. Xia,<sup>a</sup> J. Fedie,<sup>a</sup> S. Kannan,<sup>b</sup> A. Ferrier,<sup>a</sup>  
S. Rao<sup>b</sup> and M. Tanasova<sup>ib</sup>\*<sup>a</sup>

**The specificity of carbohydrate transporters towards their substrates poses a significant challenge for the development of molecular probes to monitor sugar uptake in cells for biochemical and biomedical applications. Herein we report a new set of coumarin-based fluorescent sugar conjugates applicable for the analysis of fructose uptake due to their free passage through the fructose-specific transporter GLUT5. The reported probes cover a broad range of the fluorescence spectrum providing essential tools for the evaluation of fructose transport capacity in live cells.**

Facilitative glucose transporters (GLUTs) perform gradient dependent influx and efflux of carbohydrates to sustain the nutritional needs for cell proliferation.<sup>1</sup> Metabolic deregulations in cells induce alterations in the cellular GLUT composition, resulting in overexpression of intrinsic or expression of extrinsic GLUTs.<sup>2–4</sup> Among GLUTs, glucose-transporting GLUT1 attracted attention for half a century as a target for cancer therapy and diagnostics, and other GLUTs started to gather much interest recently because of their direct relationship with cancer.<sup>3</sup> Particular attention is drawn by fructose-transporting GLUTs and the fructose-specific transporter GLUT5 due to the links between fructose uptake and cancer development, progression, and metastasis.<sup>5</sup> Consequently, the fructose transport-targeting probes are of interest as biochemical and biomedical tools.

Analyses of GLUT expression and activity as means to assess the metabolic state of the cell have been approached through the development of GLUT-targeting radiolabeled sugar analogs, as well as affinity labels.<sup>6</sup> Among radiolabeled analogs, halogenated sugar derivatives were accessed to evaluate glucose and fructose transport efficiency in conjunction with and independently of phosphorylation.<sup>6</sup> The development of fluorescently labeled

GLUT probes has been approached to alleviate the practical limitations associated with radiolabeling and to obtain high-affinity probes. Among fluorescent GLUT probes, 7-nitrobenzofurazan (NBD) has been utilized for GLUT transport analysis in the form of sugar conjugates.<sup>7–9</sup> Among those, fructose and 2,5-anhydro-D-mannitol were accessed as probes to target fructose transport providing a precedent for distinguishing GLUT5-expressing vs. GLUT5-deficient cell lines.<sup>8,9</sup> Recently, coumarin and resorufin conjugates of glucose have been evaluated as probes for glucose GLUTs.<sup>10</sup> The probes showed a limited passage through GLUTs, and accumulated in cells through non-GLUT-mediated transport.<sup>11</sup> The challenge in passing a non-natural moiety through GLUTs is also reflected by the loss of GLUT-mediated uptake for glucose–drug conjugates,<sup>12</sup> with the position of functionalization and possible change in transporter–probe interaction due to alterations in H-bonding being key players.<sup>6,13</sup>

Herein we report a set of 2,5-anhydro-D-mannitol–coumarin-based GLUT5-specific probes – ManCous – amenable for the direct analysis of GLUT5 activity in cells and signal reporting over a broad range of the fluorescence spectrum. The specific targeting of GLUT5 enables a significant differentiation in imaging of GLUT5-expressing cells vs. GLUT5-deficient cells. The range of fluorescence colors allows flexibility in conducting evaluation of GLUT5 uptake efficiency in the presence of fluorescent reporters of other cellular processes, including glucose metabolism, by mismatching probe fluorescence excitation and emission.

To access multicolor fluorescent probes compatible with GLUT-mediated uptake, we focused on coumarins as fluorophores. The choice was based on their small size and the potential to tune fluorescence color through coumarin core functionalization. The passage of 7-aminocoumarin in the form of a glucosamine conjugate through glucose GLUTs has been demonstrated,<sup>10</sup> providing a basis for testing this fluorophore as a substrate for GLUT5. Thus, as a proof-of-principle, we have investigated the uptake of a 7-aminocoumarin as a conjugate of GLUT5-targeting 2,5-anhydro-D-mannose.<sup>9,14</sup> The 7-aminocoumarin (Cou1) was synthesized from 7-hydroxycoumarin according to

<sup>a</sup> Department of Chemistry, Michigan Technological University, 1400 Townsend Drive, Houghton, Michigan 49331, USA. E-mail: mtanasov@mtu.edu

<sup>b</sup> Department of Biomedical Engineering, Michigan Technological University, 1400 Townsend Drive, Houghton, Michigan, 49331, USA

† Electronic supplementary information (ESI) available: Tables and figures, compound synthesis and characterization, NMR spectra. See DOI: 10.1039/c7cc09809j

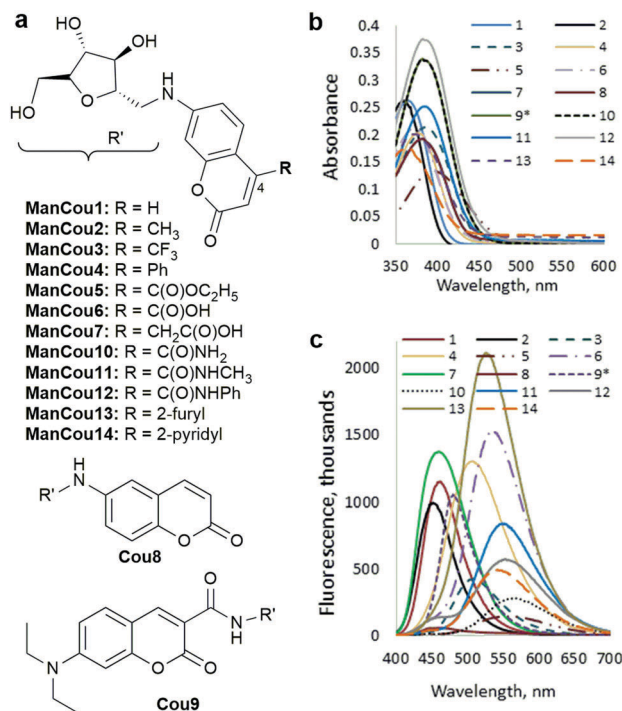


**Fig. 1** Structure and spectroscopic properties of ManCou probes. (a) Structures of ManCous 1–14; (b) UV-vis spectra for ManCous 1–14; and (c) fluorescence spectra for ManCous 1–14, exc. 385 nm. All spectra were taken for the 20  $\mu$ M ManCou conjugate. \*For clarity of representation, the UV spectrum for **ManCou9** is reported for 10  $\mu$ M concentration.

the established procedure<sup>15</sup> and conjugated to 2,5-anhydro-D-mannitol (Man) through reductive amination with 2,5-anhydro-2-carbaldehyde-D-mannitol to produce the first blue-fluorescent D-mannitol-coumarin conjugate **ManCou1** (Fig. 1a).<sup>16</sup>

With the blue-fluorescent **ManCou1** probe in hand, we moved into testing its uptake in MCF7 cells known to express GLUT5.<sup>8,17</sup> After treating MCF7 cells with various concentrations of **ManCou1**, a significant accumulation of the coumarin-induced blue fluorescence was observed after a short 10 min incubation (Fig. S1, ESI<sup>†</sup>). We found that concentrations  $\geq 20 \mu$ M were sufficient to monitor the probe accumulation through microscopy or with a plate reader.

Considering that the ManCou conjugate represents a merging of a hydrophilic sugar and a hydrophobic fluorophore, we have investigated the contribution from GLUTs vs. passive diffusion to the observed cellular accumulation of this probe. The comparative analysis of the unconjugated 7-aminocoumarin (20  $\mu$ M, 10 min, 37  $^{\circ}$ C) in MCF7 cells showed  $\sim 10$ -fold lower accumulation (Fig. 2b), highlighting a significant contribution from the sugar moiety to the observed ManCou uptake. The acquired fluorescence was primarily from the coumarin association with the cell membrane, as evident from the Z-stack analysis of Cou1-treated MCF7 cells (Fig. S1c, ESI<sup>†</sup>). While the **ManCou1** uptake was concentration-dependent, the uptake levels for the unconjugated coumarin Cou1 were not affected by the concentration (Fig. S1d, ESI<sup>†</sup>). The concentration-dependent uptake and the unambiguous contribution from the sugar moiety to the enhanced uptake

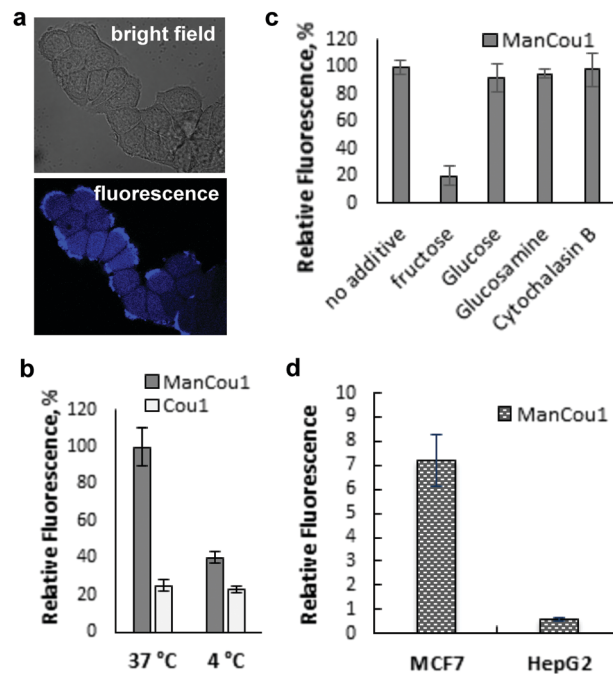


**Fig. 2** **ManCou1** (20  $\mu$ M) uptake analysis. (a) Confocal Z-stack images of MCF7 cells treated with **ManCou1** for 10 min at 37  $^{\circ}$ C; (b) comparative uptake of equimolar **ManCou1** and **Cou1** at 37  $^{\circ}$ C and 4  $^{\circ}$ C; and (c) **ManCou1** (20  $\mu$ M) uptake in the presence of 50 mM fructose, glucose, and glucosamine and 200  $\mu$ M cytochalasin B. Data collected with a fluorescence plate reader (exc/em 360 nm/430 nm) in a 96-well plate format. (d) Comparative analysis of **ManCou1** uptake in MCF7 vs. HepG2 cells. Data collected through quantification (ImageJ) of whole-cell fluorescence (obtained with an EVOS optical microscope, exc/em 405 nm/461 nm, 20 $\times$  objective) after background subtraction. All plots represent average data from triplicate measurements. Error bars represent the standard deviation between triplicate experiments.

provided a basis to consider the GLUT-mediated transport as a primary uptake mechanism for **ManCou1**. The GLUT participation became further evident from the loss of **ManCou1** uptake after incubating MCF7 cells at 4  $^{\circ}$ C (Fig. 2b) – conditions known to decrease cell metabolism and thereby GLUT-mediated uptake.<sup>8</sup> In contrast, low temperatures did not impact the uptake of Cou1, highlighting its passive diffusion through the membrane into the cell. The loss of the uptake at low temperature was also observed for higher concentrations of **ManCou1** (Fig. S1e, ESI<sup>†</sup>), suggesting the involvement of GLUT uptake even at elevated concentrations.

We have further used a series of competitive uptake and inhibition analyses to verify the uptake of **ManCou1** through GLUTs, and particularly through GLUT5. We have observed that the uptake of **ManCou1** is effectively inhibited by fructose (Fig. 2c and Fig. S2a, ESI<sup>†</sup>), suggesting the probe to be taken through fructose-transporting GLUT(s). The  $K_d = 3.1$  mM (Fig. S2b, ESI<sup>†</sup>) measured for fructose fits within the low micromolar binding range established for other GLUT5-proficient cell lines or the isolated protein.<sup>14,18</sup> When glucose and glucosamine (specific for GLUT2<sup>19</sup>) were used as competitive inhibitors, no alterations in the **ManCou1** uptake were observed (Fig. 2c and d), indicating the lack of contribution from glucose or non-specific fructose GLUTs, including GLUT2. The lack of **ManCou1** inhibition

in the presence of cytochalasin B (Fig. 2e), the established inhibitor of the uptake through GLUTs 1–4 ( $IC_{50} = 2\text{--}6\ \mu\text{M}$ ) but not GLUT5,<sup>20</sup> further ruled out non-specific transport, highlighting GLUT5-mediated uptake.

The GLUT5-specificity of **ManCou1** became further evident from the lack of the probe uptake in GLUT5-deficient liver carcinoma HepG2 cells (Fig. 2d). The basal levels of uptake measured for HepG2 cells arise from the association of the probe with the membrane, as no internalisation of the probe is observed in Z-stack analysis (Fig. S3, ESI<sup>†</sup>). The observed discrimination shows the feasibility to distinguish between GLUT5-expressing vs. GLUT5-deficient cells through fluorescence-based analysis with ManCous. The lack of inhibition from glucose enabled the use of **ManCou1** analysis in buffer or culture media (Fig. S2f, ESI<sup>†</sup>), providing a convenient tool for *in vitro* cell studies under nutrient-rich conditions.

With the successful delivery of a blue-fluorescent 7-amino-coumarin into the cell through GLUT5, we moved forward to testing ManCou analogues to gauge the tolerance of GLUT5 to coumarin fluorophores and gain access to probes of different fluorescence colors. The substitution at the C4 position of the 7-aminocoumarin had been shown to impact the fluorescence emission.<sup>21</sup> Thus, we constructed a focused library of ManCous (Fig. 1a) using readily available coumarin analogues (Cou) 2, 3, and 7, and extended the library by synthesizing Cou bearing various electron withdrawing groups at C4 (C4-EWG),<sup>16,22,23</sup> including new amides (Cou10–12), 2-furyl (Cou13), and 2-pyridyl (Cou14) C4-analogs. We have completed the library by adding 6-aminocoumarin (Cou8) and the C3-substituted analogue of 7-aminocoumarin Cou9 to assess the impact of alterations in the position of sugar conjugation on the ManCou uptake.

The Cou 5, 13 and 14 (Fig. 1) were synthesized through Pechmann condensation,<sup>16,22,24</sup> and Cou 10–12 were obtained from Cou5 through amidation with the corresponding amine.<sup>16</sup> Except for **ManCou9**, all ManCous were obtained through reductive amination of the corresponding Cou with 2,5-anhydro-2-carbaldehyde-D-mannitol. **ManCou9** was obtained through EDCI/HOBt-mediated amidation with 1-amino-2,5-anhydro-D-mannitol (Scheme S2, ESI<sup>†</sup>).

The obtained ManCous cover a broad range of the fluorescence spectrum (Fig. 1c and Table S1, ESI<sup>†</sup>) while maintaining excitation at a low wavelength (405 nm). The fluorescence intensity of ManCous varies with the substitution position and type, with **ManCou13** and **ManCou8** showing the highest and the lowest fluorescence intensity, respectively. The absolute quantum efficiency for all ManCou conjugates reflects the quenching effect of electron delocalization from the coumarin scaffold into the electron withdrawing substituent (Table S2, ESI<sup>†</sup>). We have also observed that the absorption maxima of ManCou conjugates have red-shifted 8–22 nm compared to the unconjugated coumarin (Table S1, ESI<sup>†</sup>). In an effort to explain the changes in the absorption, density functional theory was employed. The structures of 7-aminocoumarins and the corresponding ManCou conjugates were first geometrically relaxed, and then single point energy calculations were performed. The analysis of the HOMO and LUMO energies revealed a reduction

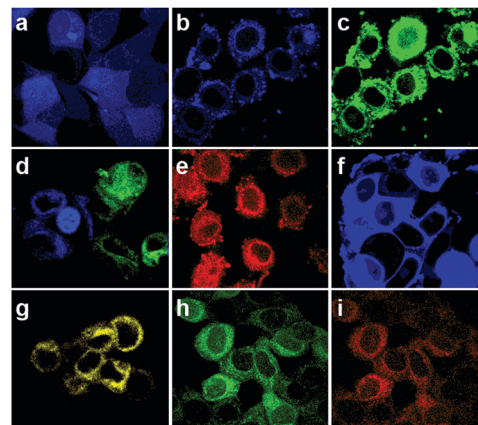


**Fig. 3** Fluorescence confocal Z-stack images of MCF7 cells treated with: (a) **ManCou2**; (b and c) **ManCou3**; (d) **ManCou4** (blue and green merge); (e) **ManCou5**; (f) **ManCou9**; and (g–i) **ManCou11**. Blue fluorescence measured at 461 nm; green fluorescence measured at 525 nm; and red fluorescence measured at 585 nm. ManCous were excited with a 405 nm laser. The yellow color was assigned considering the fluorescence maxima for ManCous 10–12. Images taken with 60 $\times$  objective after treating the cells with 20  $\mu\text{M}$  ManCous over 10 min. Images were recorded at the same laser intensity and exposure time.

of the energy gap upon alkylation of the exocyclic amine (Table S1, ESI<sup>†</sup>) expectedly contributing to the shift of the  $\lambda_{\text{max}}$  to the lesser energy.

Through confocal imaging, we have observed that MCF7 cells gained fluorescence after treatment with all ManCous except for ManCous 6 and 7 – both bearing carboxylic acid moieties. The gained cell fluorescence for ManCous 2, 8 and 9 (blue filter) highlighted the tolerance of GLUT5 towards positional isomers of coumarin–mannitol conjugates. ManCous 3 and 4 were visible under both green and blue filters; **ManCou5** was visible under orange/red filters (Fig. 3) and ManCous 10–14 were visible under red, yellow, and green filters (Fig. 3). While taken up by MCF7 cells, ManCous 2–14 did not enter HepG2 cells suggesting that coumarin modification did not impact their GLUT5-specificity (Fig. S3, ESI<sup>†</sup>). The GLUT5-specificity was also supported by the lack of uptake inhibition in the presence of glucose, glucosamine, cytochalasin B or the complete culture medium (Fig. S2, ESI<sup>†</sup>). The inhibitory effect of fructose was strong for ManCous 2, but decreased for EWG-substituted ManCous.

The Z-stack analysis of ManCou-treated MCF7 cells revealed an apparent impact of coumarin substitution on the cellular distribution of the probe. Namely, while ManCous 1 and 2 were distributed throughout the cell, C4-EWG ManCous and ManCous 8 and 9 accumulated in the cytosol (Fig. 3). The cytosolic distribution could be readily delineated through the labelling of the cell nucleus and the cell membrane with dyes of contrast fluorescence color (Fig. S4, ESI<sup>†</sup>). The differences in cellular accumulation of ManCous paralleled the differences in their uptake. Thus, while linear uptake was observed for ManCous 1 and 2 at 1–500  $\mu\text{M}$  concentrations, the uptake for all other ManCous saturated after 200  $\mu\text{M}$  (Fig. S1a, ESI<sup>†</sup>). Considering that the continuity of the uptake through GLUTs is coupled with phosphorylation,<sup>25–27</sup> it is feasible that the differences in the

uptake behaviour between ManCous could be reflecting the impact of coumarin substitution on the phosphorylation of 2,5-anhydro-D-mannitol by cellular kinases.<sup>28,29</sup>

All saturable ManCous showed  $K_d$  in the 54–75  $\mu\text{M}$  range (Fig. S5, ESI<sup>†</sup>). Considering that no saturation was observed for **ManCou1** uptake even at elevated 5 mM concentrations, we used a fructose:**ManCou1** ratio measured to induce 50% **ManCou1** uptake inhibition (Fig. S2b, ESI<sup>†</sup>) to estimate a 156-fold higher affinity for **ManCou1**. Overall, the presence of EWG groups at the coumarin appears to contribute to the strength of the ManCou–GLUT5 interaction as well as uptake rates (Fig. S5e, ESI<sup>†</sup>). This contribution is manifested by the apparent inhibition of **ManCou1** uptake in the presence of **ManCou3**. Namely, incubating MCF7 cells with the equimolar mixture of ManCous **1** and **3** resulted in the loss of nuclear accumulation of the blue fluorescence, a feature characteristic for **ManCou1**. To explore this effect further, we have employed the GLUT5-targeting green fluorescent NBDM probe ( $K_d = 22 \mu\text{M}$ ).<sup>6</sup> After incubating MCF7 cells with the equimolar mixture of **ManCou3** and NBDM, a trace of NBDM-induced green fluorescence was observed inside the cell. In contrast, **ManCou3**-induced blue fluorescence was abundant (Fig. S6a, ESI<sup>†</sup>). For the **ManCou1**–NBDM mixture, the uptake of both was observed, although the total fluorescence intensities were significantly diminished (Fig. S6b, ESI<sup>†</sup>). Overall, the differential effect of ManCous **1** and **3** on NBDM appears to reflect the differences in the strength of the GLUT5–ManCou interaction. It should be noted that the uptake of the glucose-GLUT-targeting green fluorescent NBDG probe (NBD conjugate of glucose<sup>7</sup>) was not impacted by any of the ManCou conjugates (Fig. S6c and d, ESI<sup>†</sup>). This observation further validates the GLUT5-specificity of ManCou conjugates.

In conclusion, we have shown that the fructose-specific transporter GLUT5 is capable of passing coumarins as an imaging cargo, emphasising a capacity for these facilitative transporters to pass non-native moieties in the form of an appropriate sugar or a sugar mimic conjugate. The focused coumarin library conjugated to the 2,5-anhydro-D-mannitol (ManCous) includes fluorescent probes that emit at different parts of the fluorescence spectrum, while maintaining the same excitation. As GLUT5 reporters, the probes allow for a visual discrimination between GLUT5-proficient and GLUT5-deficient cells. The structure–uptake relationship established with ManCou analogs revealed that the presence of a carboxylate moiety compromises GLUT5-mediated uptake, while ester, amide, and free amine functionalities are well tolerated. Also, a strict relationship of uptake saturation and cytosolic accumulation with coumarin substitution was observed. The spectral versatility of ManCou probes allows for combination studies through mismatching fluorescence colors of different reporters, such as nuclear and membrane dyes. Furthermore, variations of fluorescence colors within the ManCou library provide an opportunity for co-analysis of GLUT5 and other GLUTs (or other cellular targets). Considering a direct impact from ManCous on fructose uptake, further evaluation is in progress to identify the cellular

fate of ManCous and reveal their processivity by cellular kinases and their potential role as kinase inhibitors.

The research reported in this publication was supported by the Michigan Technological University and Portage Health Foundation under Award Number R01563 to M. Tanasova.

## Conflicts of interest

The authors declare no competing financial interest.

## Notes and references

- 1 A. R. Manolescu, K. Witkowska, A. Kinnaird, T. Cessford and C. Cheeseman, *Physiology*, 2007, **22**, 234–240.
- 2 M. Mueckler and B. Thorens, *Mol. Aspects Med.*, 2013, **34**, 121–138.
- 3 K. Adekola, S. T. Rosen and M. Shanmugam, *Curr. Opin. Oncol.*, 2012, **24**, 650–654.
- 4 A. M. Navale and A. N. Paranjape, *Biophys. Rev.*, 2016, **8**, 5–9.
- 5 D. T. McQuade, M. B. Plutschack and P. H. Seeberger, *Org. Biomol. Chem.*, 2013, **11**, 4909–4920.
- 6 M. Tanasova and J. Fedie, *ChemBioChem*, 2017, **18**, 1774–1788.
- 7 C. H. Zou, Y. J. Wang and Z. F. Shen, *J. Biochem. Biophys. Methods*, 2005, **64**, 207–215.
- 8 J. Levi, Z. Cheng, O. Gheysens, M. Patel, C. T. Chan, Y. B. Wang, M. Namavari and S. S. Gambhir, *Bioconjugate Chem.*, 2007, **18**, 628–634.
- 9 M. Tanasova, M. Plutschack, M. E. Muroski, S. J. Sturla, G. F. Strouse and D. T. McQuade, *ChemBioChem*, 2013, **14**, 1263–1270.
- 10 Y. Otsuka, A. Sasaki, T. Teshima, K. Yamada and T. Yamamoto, *Org. Lett.*, 2016, **18**, 1338–1341.
- 11 A. Sasaki, K. Nagatomo, K. Ono, T. Yamamoto, Y. Otsuka, T. Teshima and K. Yamada, *Hum. Cell*, 2016, **29**, 37–45.
- 12 E. C. Calvaresi and P. J. Hergenrother, *Chem. Sci.*, 2013, **4**, 2319–2333.
- 13 O. M. Soueidan, T. W. Scully, J. Kaur, R. Panigrahi, A. Belovodskiy, V. Do, C. D. Matier, M. J. Lemieux, F. Wuest, C. Cheeseman and F. G. West, *ACS Chem. Biol.*, 2017, **12**, 1087–1094.
- 14 A. Tatibouet, J. Yang, C. Morin and G. D. Holman, *Bioorg. Med. Chem.*, 2000, **8**, 1825–1833.
- 15 J. Z. Yu, Y. T. Wang, P. Z. Zhang and J. Wu, *Synlett*, 2013, 1448–1454.
- 16 see the ESI<sup>†</sup> for details.
- 17 S. P. Zamora-Leon, D. W. Golde, I. I. Concha, C. I. Rivas, F. DelgadoLopez, J. Baselga, F. Nualart and J. C. Vera, *Proc. Natl. Acad. Sci. U. S. A.*, 1996, **93**, 1847–1852.
- 18 N. Nomura, G. Verdon, H. J. Kang, T. Shimamura, Y. Nomura, Y. Sonoda, S. A. Hussien, A. A. Qureshi, M. Coincon, Y. Sato, H. Abe, Y. Nakada-Nakura, T. Hino, T. Arakawa, O. Kusano-Arai, H. Iwanari, T. Murata, T. Kobayashi, T. Hamakubo, M. Kasahara, S. Iwata and D. Drew, *Nature*, 2015, **526**, 397–401.
- 19 M. Uldry, M. Ibberson, M. Hosokawa and B. Thorens, *FEBS Lett.*, 2002, **524**, 199–203.
- 20 A. Carruthers and A. L. Helgersson, *Biochemistry*, 1991, **30**, 3907–3915.
- 21 X. G. Liu, Z. C. Xu and J. M. Cole, *J. Phys. Chem. C*, 2013, **117**, 16584–16595.
- 22 P. Reszka, R. Schulz, K. Methling, M. Lalk and P. J. Bednarski, *ChemMedChem*, 2010, **5**, 103–117.
- 23 Y. Kanaoka, A. Kobayashi, E. Sato, H. Nakayama, T. Ueno, D. Muno and T. Sekine, *Chem. Pharm. Bull.*, 1984, **32**, 3926–3933.
- 24 M. Tasiar, I. Deperasinska, K. Morawska, M. Banasiewicz, O. Vakuliuk, B. Kozankiewicz and D. T. Gryko, *Phys. Chem. Chem. Phys.*, 2014, **16**, 18268–18275.
- 25 R. J. Naftalin and R. J. Rist, *Biochem. J.*, 1989, **260**, 143–152.
- 26 R. J. Naftalin and P. M. Smith, *Biochim. Biophys. Acta*, 1987, **897**, 93–111.
- 27 P. K. Gasbjerg and J. Brahm, *Biochim. Biophys. Acta*, 1991, **1062**, 83–93.
- 28 P. T. Riquelme, M. E. Wernette-Hammond, N. M. Kneer and H. A. Lardy, *J. Biol. Chem.*, 1984, **259**, 5115–5123.
- 29 R. L. Hanson, R. S. Ho, J. J. Wiseberg, R. Simpson, E. S. Younathan and J. B. Blair, *J. Biol. Chem.*, 1984, **259**, 218–223.